Peripheral Artery Composition Evaluated With OCT

Optical coherence tomography is poised to deliver the same high-resolution imaging of the peripheral vasculature as it has in the coronary arteries.

BY J. JACOB MANCUSO, MD; KIRAN CHERUKU, MD; NATE J. KEMP, PHD; THOMAS MILNER, PHD; CHRISTOPHER BANAS; FERMIN TIO, MD; AND MARC D. FELDMAN, MD

Optical coherence tomography (OCT) is an intravascular imaging technology capable of providing high-resolution, cross-sectional images of arterial structure and pathology. Often compared with intravascular ultrasound (IVUS), OCT can better identify structures of the arterial wall, such as the internal and externalelastic laminae (IEL and EEL),[1,2] as well as provide precise measurement of the intimal thickness separate from the medial layer.[3] Additional studies have demonstrated OCT's ability to differentiate the composition of atherosclerotic plaque into fibrous, lipid-rich, and calcified tissues with sensitivity comparable to IVUS.[1,4,5] Further, with its higher resolution in the range of 10 to 20 µm (compared to 100 µm of IVUS), OCT can identify the components of vulnerable atherosclerotic plaques, including fibrous cap thickness and lipid core size.[6] Lastly, when imaging plaques with heavy calcification, OCT is less hindered by saturation artifact and acoustic shadowing than IVUS, which prevents IVUS imaging of adjacent regions and visualization of tissue behind regions of calcification.[1,7]

Although there have been numerous studies demonstrating OCT's diagnostic capacity in coronary arteries, there has been little published regarding the use of OCT in the evaluation of peripheral arteries. Peripheral arteries are classified as either elastic arteries (aorta and its great branches: carotid, iliacs, and pulmonary) or muscular arteries (coronary, renal, and popliteal). Elastic arteries have a significant amount of elastin within the tunica media; however, in muscular arteries, elastin is limited to the IEL and EEL.[8] Meissner et al showed that OCT was capable of identifying the different plaque components of crural arteries

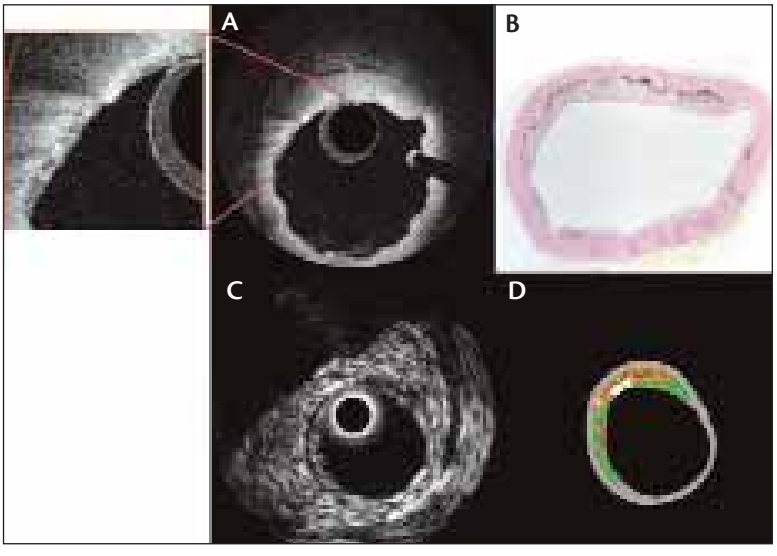

Figure 1. Microcalcification of plaque. In vivo Watanabe heritable hyperlipidemic rabbit aorta showing the speckled bright microcalcifications as identified with OCT (A, plus magnified insert); von Kossa histology confirming presence of plaque microcalcification (B); grayscale and virtual histology IVUS images displaying a "smearing" of the microcalcification, and the inability of sound to identify microcalcifications (C and D, respectively). Because the IR of calcium hydroxyapatite is high at 1.65 and that of cholesterol is close to 1.33 due to its high water content, the microcalcifications appear as bright speckles in the OCT image.

with the same high sensitivity and specificity demonstrated with coronaries.[9] Van der Meer et al described the ability of a high-resolution OCT system to identify the elastin fibers visible in the tunica media of a rat aorta while proving the technology's ability to produce detailed images of various peripheral arteries in pigs, rats, and humans.[10] However, both of these studies are limited in that they were performed on ex vivo tissue.

In this article, we provide examples of OCT's ability to visualize peripheral vessels in vivo. First, we show the OCT appearance of the elastin distribution within the layers of a porcine iliac artery. Further, we demonstrate the appearance of microcalcifications within the plaque of an atherosclerotic rabbit aorta visualized with OCT compared to imaging with both grayscale and virtual histology IVUS.

METHODS

Optical Coherence Tomography System

The prototype Volcano OCT imaging system (Volcano Corporation, San Diego, CA) consists of a disposable 3-F catheter, patient interface module (PIM), and upright imaging console. The frequency-domain OCT system is based on a tunable laser source centered at 1,310-nm wavelength and provides an A-scan rate of 20 kHz and axial resolution of approximately 10 µm. Advanced signal processing provides real-time acquisition and display of OCT images at 20 fps (1,000 A-lines/frame).

Watanabe Rabbit Aorta

All animal experiments were approved by the Institutional Animal Care and Use Committee of the University of Texas Health Science Center at San Antonio. A 3.5-year-old Watanabe heritable hyperlipidemic rabbit was sedated, and a 6-F femoral arterial sheath was inserted. A guidewire was advanced into the abdominal aorta, and its location was verified with fluoroscopy. The OCT catheter was advanced over the guidewire, and several 20-mm pullbacks were performed during infusion of 0.9% saline through the femoral sheath. After OCT imaging, an IVUS catheter was advanced over the same guidewire, and 20-mm pullbacks of the identical region of the abdominal aorta were performed. After completion of the experiment, the rabbit was euthanized, and the aorta and heart were removed. The left ventricle was cannulated and pressure-perfused with formalin solution for 30 minutes. The region of the aorta that was imaged was then sent for histology sectioning and stained with von Kossa calcium stains.

Imaging of Porcine Coronary and Iliac Arteries

OCT images were obtained of coronary and iliac arteries of two Sus scrofa pigs. In both experiments, the pig was sedated and placed on mechanical ventilation. Cutdown procedures of the right femoral artery were performed, and 6-F arterial sheaths were placed inside the femoral arteries. In one pig, a 6-F hockey stick guiding catheter was advanced through the aorta to the ostia of the coronary arteries. After guide catheter placement, which was verified with fluoroscopy and contrast injection, a guidewire was advanced through the guiding catheter serially into each of the coronary arteries to be imaged. The OCT catheter was advanced over the guidewire, and pullbacks were performed of each of the coronary arteries during infusion of 0.9% saline. In the second pig, a guidewire was advanced into the left iliac artery, and the OCT catheter was advanced over the guidewire. OCT images were then obtained of the iliac artery during hand injection of 0.9% saline. At the end of both experiments, the pigs were euth-

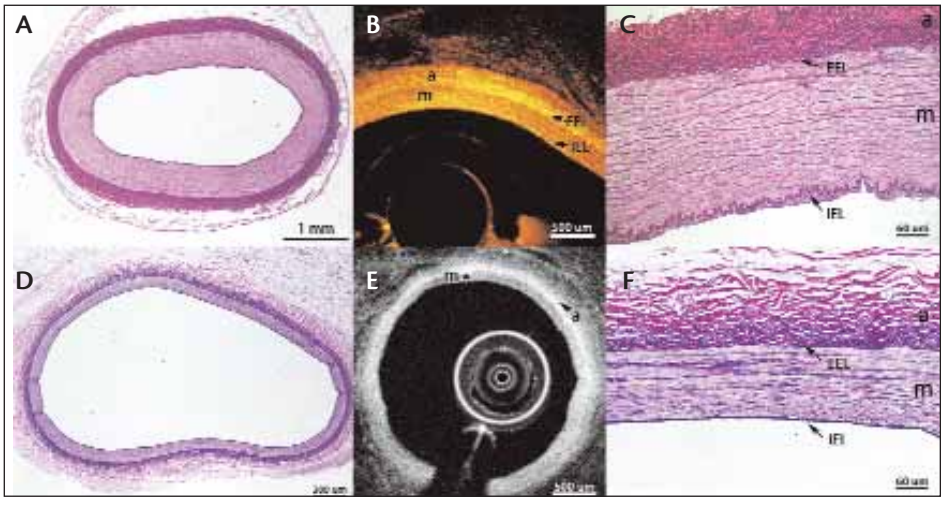

Figure 2. Comparison of in vivo OCT images and histology between elastic (iliac) and muscular (coronary) porcine arteries. Histology of the iliac artery stained for elastin (Verhoeff-van Gieson) (A) and corresponding OCT image (B). Higher magnification of the iliac arterial wall (C) demonstrates the high density of elastin fibers throughout the tunica media (m) and elastic-rich portion of the tunica adventitia (a), which are also evident in the OCT image. Also illustrated are the IEL and EEL. Histology of coronary artery stained for elastin (D) and corresponding OCT image (E). Higher magnification of the coronary arterial wall (F) reveals less elastin fibers in the tunica media, which is also evident in the corresponding OCT image.

Figure 3. High-resolution, ex vivo OCT image (A) and corresponding histology (B) of rat aorta. The individual elastin fibers of this elastic artery are visualized in the tunica media with both histology and OCT (a=tunica adventitia and m=tunica media). (Reprinted with permission from van der Meer et al. Lasers in Medical Science. 2005; 20:45-51.[10])

anized, and the coronary and iliac arteries were pressure perfused with formalin. Histology sections of the arteries were then stained with Verhoeff-van Gieson elastin stains.

RESULTS

OCT images obtained of the rabbit aorta were consistent with microcalcifications, having the appearance of speckled bright "spots" during OCT interrogation (Figure 1A). This speckled pattern correlated with the microcalcification pattern seen with von Kossa-stained histologic sections (Figure 1B). IVUS images obtained of the same aortic region, however, were not able to detect the microcalcifications seen with OCT and histology. Rather, IVUS showed significant saturation artifact, as well as acoustic shadowing, behind the region of calcification. This "smeared" appearance of calcification with IVUS was apparent with both grayscale imaging as well as virtual histology (Figures 1C and 1D).

OCT images obtained of the porcine iliac and coronary arteries demonstrated the structural components of the arterial wall, which correlated with elastin (Verhoeff-van Gieson) stain on histology. Regions with high elastin content are more signal-rich on OCT images. Visualization of the IEL, the tunica media, the EEL, as well as the elastin-rich portion of the tunica adventitia, was apparent with both OCT and histology for the iliac artery (Figures 2A and 2B) and coronary artery (Figures 2D and 2E). The differences between the iliac and coronary artery histology can best be appreciated at higher magnification (Figures 2C and 2F): the thicker tunica media and tunica adventitia layers of the iliac with more elastin fibers in the tunica media layer are readily apparent with histology and also identified with OCT (Figures 2B and 2E).

DISCUSSION

Microcalcification has been identified as one of several features found in vulnerable atherosclerotic plaque. Although IVUS is capable of identifying large calcium deposits with high sensitivity, the technology is incapable of reliably identifying regions of arterial microcalcifica-

tion.[11] IVUS does not have the image resolution to discern microcalcifications but rather "smears" them, providing an artificial appearance of coalesced regions of calcification.

Previous studies of the OCT appearance of calcification published by other groups have identified fibrocalcific plaques, which have the appearance of calcium nodules.[1,2,7] Our group, however, was the first to describe the OCT appearance of arterial microcalcification patterns in ApoE -/- mice.[6] The large index of refraction (IR) gradient between calcium hydroxyapatite (1.65 IR) mixed with lipid (1.33 IR) results in bright speckles in the OCT image. These bright speckles are consistent with the microcalcifications seen on von Kossa staining, and their identification is consistent with the higher resolution of OCT.[12] In the current study, we have extended these findings into a larger animal model with an invasive catheter system for the first time.

The ability of OCT to visualize the elastin content of the arterial wall is evident in the current study. In ex vivo studies, OCT has demonstrated the ability to visualize the elastin distribution of elastic, peripheral arteries with brighter signal in regions of high elastin content with a high-resolution system able to visualize individual elastin fibers within the tunica media (Figure 3).[10] We have provided an in vivo demonstration of the ability of OCT to differentiate the three layers of the arterial wall in an elastic, peripheral artery. We anticipate future development of higher-resolution OCT systems with polarization sensitivity, which may further improve the ability to visualize the components of the peripheral arterial wall.

Current intravascular OCT systems available commercially have been designed for use in coronary arteries and thus are not optimal for use in the larger-diameter peripheral vessels. Systems optimized for use in peripheral arteries will require a longer focal length so that the entire circumference of artery can be imaged in real time. The iliac image shown in Figure 2 was obtained with the prototype Volcano OCT catheter, which was designed for coronary arteries, and thus the entire circumference of the porcine iliac artery is not apparent.

CONCLUSION

It is anticipated that OCT systems will be constructed for imaging peripheral vessels, which will maintain the same enhancement of image resolution that has been apparent in coronary OCT imaging to date. ■

Acknowledgments: This study was supported by a grant from Volcano Corporation.

J. Jacob Mancuso, MD, is a Fellow in the Division of Cardiology at the University of Texas Health Science Center, San Antonio, Texas. Financial interest disclosure information was not available at the time of publication. Dr. Mancuso may be reached at mancuso@uthscsa.edu.

Kiran Cheruku, MD, is an Interventional Fellow in the Division of Cardiology at the University of Texas Health Science Center, San Antonio, Texas. Financial interest disclosure information was not available at the time of publication. Dr. Cheruku may be reached at cheruku@uthscsa.edu.

Nate J. Kemp, PhD, is Senior Engineer in the OCT Division of Volcano Corp., San Antonio, Texas. Financial interest disclosure information was not available at the time of publication. Dr. Kemp may be reached at nkemp@volcanocorp.com.

Thomas Milner, PhD, is a Professor in the Department of Biomedical Engineering at the University of Texas, Austin, Texas. Financial interest disclosure information was not available at the time of publication. Dr. Milner may be reached at milner@mail.utexas.edu.

Christopher Banas is President of the OCT Division of Volcano Corp., San Antonio, Texas. Financial interest disclosure information was not available at the time of publication. Mr. Banas may be reached at cbanas@volcanocorp.com.

Fermin Tio, MD, is a Professor in the Department of Pathology at the University of Texas Health Science Center, San Antonio, Texas. Financial interest disclosure information was not available at the time of publication. Dr. Tio may be reached at tio@uthscsa.edu.

Marc D. Feldman, MD, is Professor of Medicine and Engineering, Director, Cardiac Catheterization Lab, University of Texas Health Science Center, San Antonio, Texas. Financial interest disclosure information was not available at the time of publication. Dr. Feldman may be reached at feldmanm@uthscsa.edu.

1. Jang IK, Bouma BE, Kang DH, et al. Visualization of coronary atherosclerotic plaques in patients using optical coherence tomography: comparison with intravascular ultrasound. J Am Coll Cardiol. 2002;39:604-609.
2. Yabushita H, Bouma BE, Houser SL, et al. Characterization of human atherosclerosis by optical coherence tomography. Circulation. 2002;106:1640-1645.
3. Kume T, Akasaka T, Kawamoto T, et al. Assessment of coronary intima-media thickness by optical coherence tomography: comparison with intravascular ultrasound. Circ J. 2005;69:903-907.
4. Huang D, Swanson EA, Lin CP, et al. Optical coherence tomography. Science. 1991;254:1178-1181.
5. Brezinski ME, Tearney GJ, Bouma BE, et al. Optical coherence tomography for optical biopsy: properties and demonstration of vascular pathology. Circulation. 1996;93:1206-1213.
6. Cilingiroglu M, Oh JH, Sugunan B, et al. Detection of vulnerable plaque in a murine model of atherosclerosis with optical coherence tomography. Catheter Cardiovasc Interv. 2006;67: 915-923.
7. Kume T, Okura H, Kawamoto T, et al. Assessment of the histological characteristics of coronary arterial plaque with severe calcification. Circ J. 2007;71:643-647.
8. Schoen FJ, Cotran RS. Blood Vessels. In: Cotran RS, Kumar V, Collins T. eds. Robbins Pathologic Basis of Disease. 6th ed. Philadelphia, PA: W.B. Saunders Co; 1999:494.
9. Meissner OA, Rieber J, Babaryka G, et al. Intravascular optical coherence tomography: comparison with histopathology in atherosclerotic peripheral artery specimens. J Vasc Interv Radiol. 2006;17:343-349.
10. van der Meer FJ, Faber DJ, Perree J, et al. Quantitative optical coherence tomography of arterial wall components. Lasers in Medical Science. 2005;20:45-51.
11. Friedrich GJ, Moes NY, Mühlberger VA, et al. Detection of intralesional calcium by intracoronary ultrasound depends of histological pattern. Am Heart J. 1994;128:435-441.
12. Cilingiroglu M, Oh JH, Sanghi PK, et al. Clinical lessons from OCT imaging of Apo E knockout mice. In: Regar E, van Leeuwen AMGJ, Serruys, PW, eds. Optical Coherence Tomography in Cardiovascular Research. Abingdon, Oxon, UK: Informa Healthcare; 2007:133-146.